Traffic 2013; **14:** 1091–1104

doi:10.1111/tra.12095

A *trs20* Mutation That Mimics an SEDT-Causing Mutation Blocks Selective and Non-Selective Autophagy: A Model for TRAPP III Organization†

Stephanie Brunet[1,‡], Nassim Shahrzad[1,‡], Djenann Saint-Dic[1], Hartley Dutczak[1] and Michael Sacher[1,2,*]

[1] *Department of Biology, Concordia University, Montreal, Quebec Canada*
[2] *Department of Anatomy and Cell Biology, McGill University, Montreal, Quebec Canada*

**Corresponding author: Michael Sacher, michael.sacher@concordia.ca*

† *This paper is dedicated to the memory of Noam Hirsch, a young man who was taken from his family and friends much too soon. May his memory serve as a source of inspiration to all who knew him.*

‡ *These authors contributed equally to this work.*

TRAPP is a multisubunit complex that functions in membrane traffic. Mutations in the mammalian TRAPP protein C2 are linked to the skeletal disorder spondyloepiphyseal dysplasia tarda (SEDT) that is thought to arise from an inability to secrete procollagen from the endoplasmic reticulum. Here, we show that C2 binds to the SNARE protein Syntaxin 5 and this interaction is weakened by an SEDT-causing missense mutation (D47Y). Interestingly, the equivalent mutation (D46Y) in the yeast C2 homolog Trs20p does not block anterograde traffic but did affect endocytosis. The *trs20D46Y* mutation interfered with the interaction between Trs20p and Trs85p (TRAPP III-specific subunit), Trs120p and Trs130p (TRAPP II-specific subunits). Size exclusion chromatography suggested that this yeast mutation destabilized the TRAPP III complex that is involved in autophagy. We further show that this mutation blocks both the selective cytosol-to-vacuole (cvt) pathway as well as non-selective autophagy. We demonstrate that the apparent molecular size of the TRAPP III complex is dependent upon membranes, and that the presence of TRAPP III is dependent upon Atg9p. Finally, we demonstrate that lipidated Bet3p is enriched in TRAPP III and that lipidation increases the efficiency of autophagy. Our study suggests that Trs20p acts as an adaptor for Trs85p and Trs120p and reveals complexities in TRAPP III assembly and function. The implications of C2D47Y in SEDT are discussed.

Key words: Atg9p, autophagy, Bet3p, SEDT, TRAPP, Trs20p, Trs85p

Received 5 March 2013, revised and accepted for publication 28 July 2013, uncorrected manuscript published online 30 July 2013, published online 14 August 2013

The ability of a cell to properly localize its protein complement is critical for the cell to function correctly. Referred to as membrane transport, the process is mediated by vesicle carriers that move between various compartments. There are many factors involved in ensuring the fidelity of this process and defects in this trafficking process lead to numerous disorders (1,2). Although strong defects in membrane traffic would be expected to result in embryonic lethality, more subtle mutations may lead to tissue-specific disorders.

The overall process involves tethering factors, small GTP-binding proteins of the rab family, coat proteins that encompass the transport vesicles and SNARE proteins that are involved in vesicle fusion with the target membrane (3). Intimate connections between each of these factors have been identified in various transport steps. In transport between the endoplasmic reticulum (ER) and Golgi in yeast, the tethering factor TRAPP I binds to the coat protein Sec23p, thus acting to bridge the vesicle and the target membrane (4,5). In addition, as a guanine nucleotide exchange factor (GEF), TRAPP I activates the GTPase Ypt1p (6,7). Although a direct link between TRAPP I and SNAREs has yet to be demonstrated, SNARE complex assembly is impaired in a *bet3* mutant, a gene that encodes an essential TRAPP I subunit (8). Thus, as a tethering factor, TRAPP I serves to link all of these processes to ensure proper targeting of ER-derived transport vesicles.

TRAPP I is composed of six distinct polypeptides (Bet5p, Bet3p, Trs20p, Trs23p, Trs31p and Trs33p) although the levels of Trs20p appear to be substoichiometric in this complex (9). Two related complexes called TRAPP II and III have also been described (9,10). Each complex contains the TRAPP I core along with unique polypeptides: Trs65p, Tca17p, Trs120p and Trs130p for TRAPP II and Trs85p for TRAPP III (9–12). TRAPP II has been implicated in traffic at the late Golgi, endocytosis and non-selective autophagy (9,13,14) and TRAPP III has been shown to function in selective autophagy (10,15,16). Interestingly, Trs85p, the TRAPP III-specific subunit, has been implicated in ER-to-Golgi transport as well (9,17). Because the TRAPP I core possesses Ypt1p GEF activity, both TRAPP II and III have also been shown to be capable of activating Ypt1p (9,10). Indeed, Ypt1p has been implicated in the same membrane trafficking processes as TRAPP I, II and III (10,16,18–21).

In humans, mutations in TRAPPC2 (C2), the homolog of the yeast TRAPP I core protein Trs20p, have been linked to the skeletal disorder spondyloepiphyseal dysplasia tarda (SEDT) (22). This X-linked disorder affects bone growth in the spine and the ends of long bones in the

arms and legs. Patients are of short stature and develop dysplasia of joints in the shoulders, hips and knees. The disorder appears to result from an inability of chondrocytes to secrete collagen (23). Indeed, given the size of procollagen (~300 nm) and the diameter of an ER-derived carrier (~60 nm) it has been an unanswered question as to how procollagen is transported between the ER and Golgi. Furthermore, understanding how a ubiquitously expressed protein such as C2 could lead to the phenotype seen in SEDT patients has been a major focus of researchers studying TRAPP. A recent report suggested that recruitment of C2 to ER exit sites by the procollagen receptor Tango1 regulates the cycle of the GTPase Sar1, thus allowing carriers to achieve a size sufficient to accommodate the large procollagen molecule (24).

While elegant, we speculated that the model put forth regarding the role of C2 in procollagen secretion may not explain the etiology of all SEDT mutations because yeast neither secrete collagen nor possess a readily identifiable homolog of the collagen receptor. Furthermore, C2-dependent Golgi fragmentation and collagen secretion are separable functions (24,25), suggesting C2 may have several roles in the cell. Interestingly, an SEDT-causing missense mutation at D47 in C2 (C2D47Y) cannot suppress the lethality of a yeast *trs20*Δ mutation although wild-type C2 can (26). As yeast do not produce collagen, this suggests that the D47 residue is involved in some other process. We therefore set out to characterize the interactions and function of the C2D47Y protein and its yeast homolog trs20D46Yp. Here, we demonstrate an interaction between C2 and the SNARE protein Syntaxin 5 and show that this interaction is sensitive to the D47Y mutation. In yeast, trs20D46Yp is not involved in anterograde transport but is defective in endocytosis and both selective and non-selective autophagy, correlating with a destabilization of TRAPP III. We also show that the appearance of TRAPP III is dependent upon Atg9p and that the function of TRAPP III is influenced by palmitoylation of Bet3p, suggesting unexpected complexities in TRAPP III assembly and localization.

Results

Binding of TRAPPC2 to Syntaxin 5 is dependent upon the D47 residue in TRAPPC2

A recent study suggested that C2 participates in the export of procollagen by regulating the Sar1p GTPase cycle (24). C2 is recruited to ER exit sites through an interaction with the collagen receptor Tango1. We reasoned that C2 has additional functions for the following reasons: (i) the yeast *Saccharomyces cerevisiae* has neither a recognizable Tango1 homolog nor a collagen-like molecule, yet the yeast homolog of C2 (Trs20p) is encoded by an essential gene, and (ii) the role of C2 in collagen export and Golgi morphology can be separated based on the extent of C2 knockdown (24,25). As C2 is structurally related to longin-domain-containing SNARE proteins (27–29) we speculated that it may interact with SNAREs involved in the early secretory pathway of mammalian cells. Using a yeast two-hybrid assay, we screened for interactions between C2 and the early secretory pathway SNAREs Syntaxin 5, membrin, Sec22b, Ykt6, Bet1 and GS28. As shown in Figure 1A, we detected an interaction between C2 and Syntaxin 5. The interaction was mediated through the SNARE domain of Syntaxin 5 (Figure 1B). This interaction was not due to the fact that C2 is a longin-domain-containing protein because TRAPPC1 and TRAPPC4, two other TRAPP components with longin domains, did not interact with Syntaxin 5 (Figure 1C). In an attempt to define the region of C2 that participates in the interaction with Syntaxin 5 we found that the pathogenic missense mutation D47Y in C2 found in patients with SEDT significantly weakened the interaction (Figure 1D). Mutations near D47, however, had no effect (Figure 1D).

To confirm the interaction between C2 and Syntaxin 5, we performed *in vitro* binding studies with GST-tagged Syntaxin 5 and His-tagged C2. As shown in Figure 1E, an interaction between the two proteins was detected *in vitro*. Consistent with the yeast two-hybrid assay above (Figure 1C), the D47Y mutation in C2 weakened this interaction *in vitro* (Figure 1E). As a third confirmation of this interaction we expressed myc-tagged C2 or C2D47Y in HeLa cells, immunoprecipitated Syntaxin 5 from the lysates prepared from the transfected cells and probed the immunoprecipitates for the presence of myc-C2. Consistent with the first two assays, we noted an interaction between Syntaxin 5 and C2 that was weakened by the D47Y mutation in C2 (Figure 1F).

Syntaxin 5 can be found as a component of a larger SNARE complex or free from other SNAREs (30). SNARE complex formation is increased by treatment of intact cells with *N*-ethylmaleimide (NEM) (30). To investigate whether C2 binds to Syntaxin 5 in a SNARE complex, HeLa cells were transfected with C2-myc and cells were either untreated or treated with 10 μM NEM, a concentration sufficient to lead to SNARE complex accumulation (N.S. and M.S., unpublished observation), for increasing times. Lysates prepared from the cells were immunoprecipitated with Syntaxin 5 antibody and probed for C2-myc. Untreated cells showed a small amount of C2 co-precipitating with Syntaxin 5 (Figure 1G). The amount of co-precipitating C2 increased with increasing times of NEM treatment, suggesting that C2 binds to Syntaxin 5-containing SNARE complexes. Endogenous C2 was also shown to co-precipitate with Syntaxin 5 in HeLa cells in an NEM-dependent manner (Figure 1H).

The yeast mutant trs20D46Y does not prevent processing of carboxypeptidase Y (CPY)

The human C2 D47 residue is conserved in the yeast Trs20 protein at D46. Because yeast do not secrete collagen, and because we failed to detect a similar interaction between Trs20p and the yeast Syntaxin 5 homolog Sed5p (not shown), this conserved residue

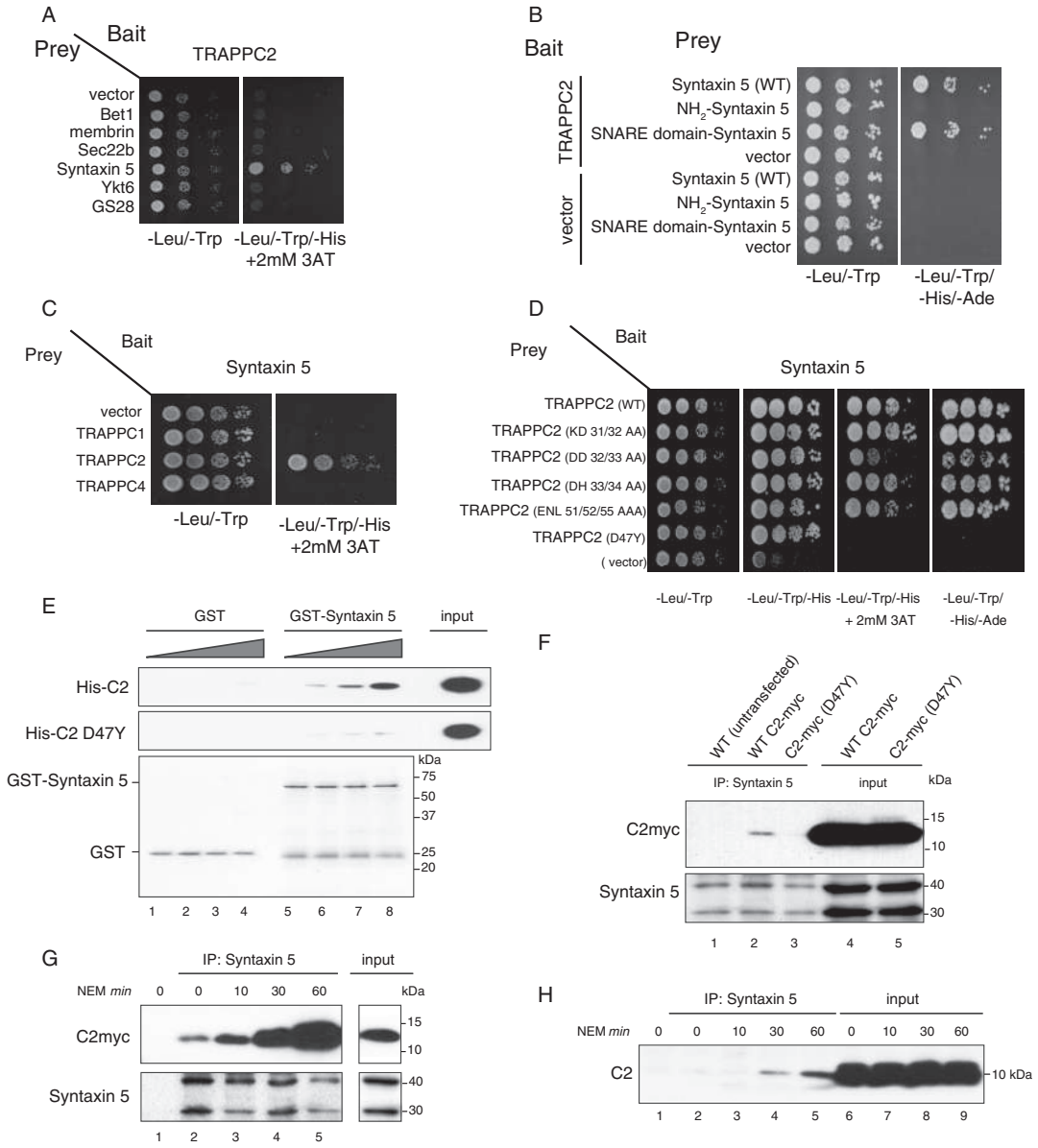

Figure 1: TRAPPC2 binds to Syntaxin 5. A) TRAPPC2 was cloned into the yeast two-hybrid vector pGBKT7 and the SNAREs indicated were cloned into pGADT7. The plasmids were transformed into AH109 and Y187 cells, mated and spotted as serial dilutions onto SD-leu/-trp and SD-leu/-trp/-his/-ade and grown at 30°C for ~3 days. B) Full-length Syntaxin 5, the SNARE domain (amino acids 263-333) or the amino-terminal domain (amino acids 1-262) of Syntaxin 5 were cloned into pGADT7 and tested for an interaction by yeast two hybrid with TRAPPC2 (or an empty pGADT7 vector control) as described in (A). C) TRAPPC2 in pGBKT7 was tested for its ability to interact with the indicated TRAPP proteins expressed in pGADT7 by yeast two hybrid. D) TRAPPC2 or the indicated mutants were inserted into pGBKT7 and tested for their ability to interact with Syntaxin 5 cloned into pGADT7 by yeast two hybrid. E) Increasing amounts of His-tagged TRAPPC2 or TRAPPC2D47Y (0, 0.05, 0.1 and 0.25 μM) were incubated with 0.5 μM GST-tagged Syntaxin 5 as indicated in *Materials and Methods*. The bound TRAPPC2 was detected by western analysis using anti-His IgG. An input representing 10% is shown. The lower panel shows a coomassie-stained gel of the bait proteins GST and GST-Syntaxin 5. F) Lysates from HeLa cells transfected with myc-tagged TRAPPC2 or TRAPPC2D47Y were treated with anti-Syntaxin 5 IgG and the immunoprecipitates were probed for the presence of myc-TRAPPC2 and Syntaxin 5 by western analysis using anti-myc or anti-Syntaxin 5 IgG. A portion (10%) of the input is also shown. G) HeLa cells were transfected with myc-tagged TRAPPC2 or TRAPPC2D47Y and then treated for increasing times (indicated) with 10 μM NEM. Lysates were prepared and Syntaxin 5 was immunoprecipitated as in (F) (lanes 2–5). Lysate in lane 1 was from a non-transfected culture. The bound, tagged TRAPPC2 was detected using anti-myc IgG and Syntaxin 5 was detected using anti-Syntaxin 5 IgG. A portion (10%) of the input is shown. H) Non-transfected HeLa cells were treated for increasing times (indicated) with 10 μM NEM. Lysates were prepared and processed as in (G). Lysate in lane 1 was not incubated with IgG during the precipitation and only received protein A-agarose beads. Endogenous TRAPPC2 was detected using anti-TRAPPC2 IgG. A portion (10%) of the input is shown.

must be involved in some other cellular process. To address this, we studied the consequences of the equivalent mutation in *TRS20* (*trs20D46Y*) in yeast. Although this mutant was slightly heat sensitive, it was not as severely compromised as *trs20ts*, a mutant that was constructed by random mutagenesis (Figure 2A). To investigate whether *trs20D46Y* blocked early secretory protein traffic, we performed a pulse-chase experiment using the vacuolar hydrolase CPY. This commonly used secretory marker protein is translated and inserted into the ER as a 'p1' form. It then traffics to the Golgi where it migrates as a slower 'p2' form before it is delivered to the vacuole as a faster migrating 'm' form (31). As shown in Figure 2B, neither *trs20D46Y* nor *trs20ts* displayed a defect in the processing of CPY. In addition, *trs85*Δ, a gene whose product has previously been reported to function in ER-to-Golgi transport but has more recently been implicated in selective autophagy, also processed CPY similar to wild type. These results suggest that *trs20D46Y* does not function in ER-to-Golgi traffic but may affect some aspect of TRAPP II and/or III activity.

The D46Y mutation in trs20 affects its interactions with TRAPP II and III proteins

To begin to understand where the D46 residue in Trs20p functions, we compared the interactions of Trs20p and trs20D46Yp with all known components of the TRAPP complex using the yeast two-hybrid assay. As shown in Figure 3A, Trs20p interacted with Trs31p, Bet3p, Trs85p, Trs120p and Trs130p (all other TRAPP subunit interactions tested were negative). The first two proteins are components of the TRAPP core and these interactions were seen in the crystal structure of both the yeast and mammalian complexes (33,34). Trs85p is a component of TRAPP III, whereas Trs120p and Trs130p are found in the TRAPP II complex. These results are consistent with a recent report suggesting that the mammalian Trs20p homolog C2 interacts with both the Trs120p (TRAPPC9) and Trs85p (TRAPPC8) homologs (35). Interestingly, while the D46Y mutation in Trs20p did not affect the interaction with neither Bet3p nor Trs31p, it did weaken the interaction between Trs20p and the TRAPP II/III-specific components Trs85p, Trs120p and Trs130p (Figure 3A).

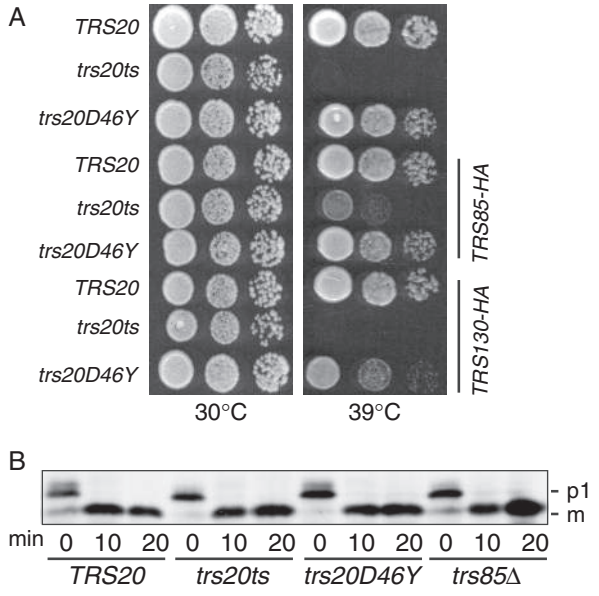

Figure 2: *trs20D46Y* does not block trafficking of CPY. A) A yeast strain with *trs20D46Y* as the sole copy of *TRS20* was spotted as a serial dilution on YPD plates and grown at either 30 or 39°C. A *trs20ts* strain (32) was also included. The same *trs20* mutations were introduced into a yeast strain with the sole copy of *TRS130* tagged with the HA epitope. B) Yeast strains indicated were pulsed with ^{35}S-methionine for 4 min and chased with unlabeled methionine for the times indicated as described in *Materials and Methods*. CPY was immunoprecipitated using anti-CPY IgG, and the forms of CPY were visualized by radioautography.

We also used yeast genetic interactions to investigate the connection between *TRS20* and the TRAPP II and III complexes. Although *trs20D46Y* is mildly heat sensitive, the phenotype was more pronounced in the presence of HA-tagged Trs130p but not with HA-tagged Trs85p (Figure 2A). Neither *trs20D46Y* nor *trs20ts* displayed genetic interactions with *trs85*Δ, although *trs20ts* was synthetically lethal with *trs65*Δ (a gene encoding a TRAPP II subunit) (Figure 3B). Finally, using the more heat-sensitive *trs20D46Y* mutation in the *TRS130-HA* background, we found that, in addition to the expected suppression conferred by *TRS20* and *TRS130*, *TRS120* was capable of suppressing the temperature-sensitive growth phenotype (Figure 3C). These results suggest that while *trs20D46Y* does not have a strong growth phenotype, it does display interactions with genes encoding TRAPP II and III subunits.

*trs20D46Y phenocopies trs85*Δ *in both GFP-Snc1p recycling and calcofluor white (CFW) hypersensitivity*

Because early secretory protein traffic was unaffected in *trs20D46Y* cells, we examined the cells for a general secretion defect. Included in these studies was the *trs85*Δ mutant as Trs20p showed a D46-dependent interaction with Trs85p (see above). Cells were pulsed with ^{35}S-methionine and then chased with cold methionine and the culture supernatant was assayed for secreted proteins. As expected, *sec18*, a gene involved in virtually all membrane trafficking steps, potently blocked the appearance of secreted proteins compared with wild type (Figure 4A). In contrast, *trs20D46Y* appeared similar to wild type, suggesting that secretion is not defective in this mutant. A similar result was seen for *trs85*Δ (Figure 4A), whereas *trs130ts* showed a partial block in secretion (not shown; see 13). A partial block in secretion was also seen in *trs20ts* (Figure 4A).

CFW sensitivity is often used as a measure of activity of the endocytic pathway (36). This compound binds to chitin in the yeast cell wall, enters the cell and ultimately results in cell death. A defect in endocytosis leads to elevated

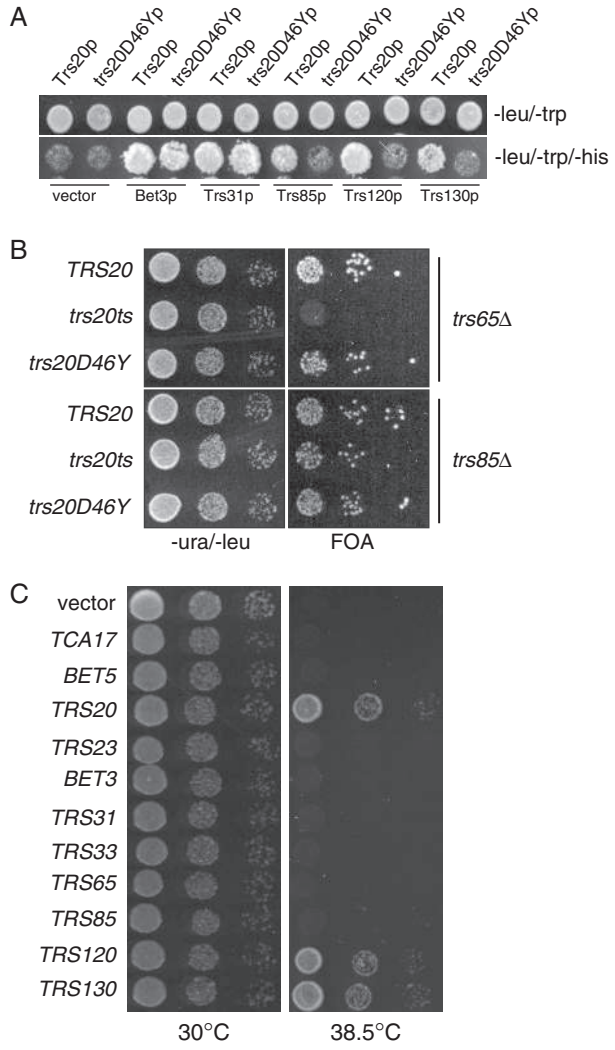

Figure 3: Genetic interactions affected by *trs20D46Y*. A) The open reading frames encoding *TRS20* and *trs20D46Y* were cloned into pGBKT7, transformed into AH109 yeast cells and mated to Y187 yeast that harbored pGADT7 containing the indicated TRAPP open reading frames. The resulting diploids were spotted onto SD-leu/-trp (top panel) or SD-leu/-trp/-his (bottom panel). B) The *trs20D46Y* mutation was introduced into a yeast strain in which the chromosomal copy of *TRS65* was deleted (*trs65*Δ) and a copy of wild-type *TRS65* was maintained on a *URA3*-based plasmid. The plasmid was counter-selected on 5-fluoroorotic acid-containing plates. C) A yeast strain (*TRS130*-HA *trs20D46Y*; see Figure 2A) was transformed with a plasmid containing the indicated TRAPP gene and grown on YPD plates at either 30 or 38.5°C.

chitin levels in the cell wall and a hypersensitivity of the cells to CFW, whereas a defect in anterograde traffic results in CFW resistance. In the case of *trs20D46Y* the cells were hypersensitive to CFW (Figure 4B). This was also the case for *trs20ts* and *trs85*Δ.

We next examined GFP-Snc1p localization in these cells. Snc1p is a SNARE protein that cycles between the

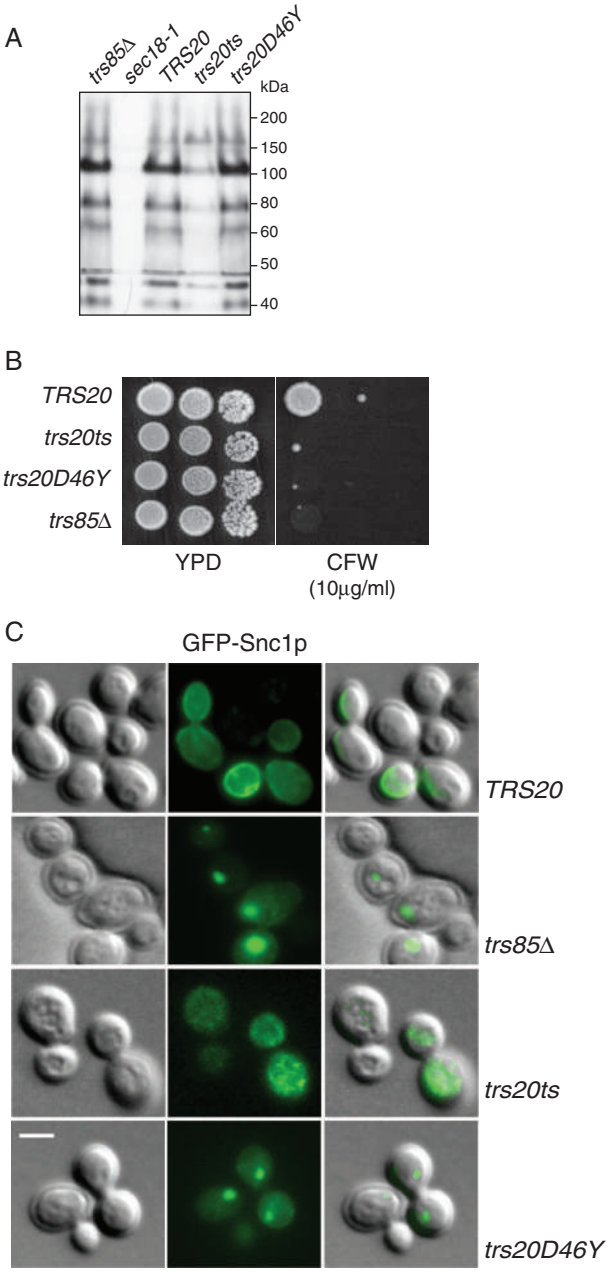

Figure 4: The effects of *trs20D46Y* and *trs85*Δ on membrane traffic pathways. A) Yeast strains indicated were pulsed with ^{35}S-methionine for 15 min and chased with unlabeled methionine for 15 min. The yeast were separated from the growth medium during a brief centrifugation and proteins in the growth medium were precipitated with trichloroacetic acid. The precipitates were visualized by radioautography. B) The indicated yeast strains were spotted as serial dilutions on YPD plates either with or without 10 μg/mL CFW and grown at 30°C. C) Yeast strains were transformed with a plasmid containing GFP-Snc1p. The cells were fixed with paraformaldehyde and the localization of GFP-Snc1p was assessed by fluorescence microscopy. Accumulation of GFP-Snc1p on internal structures is seen in 24 ± 1%, 62 ± 2%, 77 ± 1% and 89 ± 3% of wild-type, *trs20ts*, *trs20D46Y* and *trs85*Δ cells, respectively ($N = 150$ for each strain, performed in triplicate). The scale bar is 2 μm.

Golgi and plasma membrane via the endocytic pathway. When fused to GFP, the protein localizes to the plasma membrane and to small buds in dividing cells (Figure 4C). Previous studies have shown an accumulation of internal structures in *trs85*Δ cells (11,37) (Figure 4C). Similarly, we found internal, GFP-Snc1p-positive structures in *trs20D46Y* and *trs20ts*. Collectively, our results suggest that *trs20D46Y* affects post-Golgi/endosome trafficking. The similar phenotype was seen in *trs85*Δ and the interaction between Trs20p and the TRAPP III-specific component Trs85p suggests Trs20p may act in autophagy.

TRAPP III is destabilized in the trs20D46Y mutant

To better understand the trafficking step(s) affected in *trs20D46Y*, we examined the assembly state of the TRAPP complexes. First, yeast lysates from wild-type or *trs20* mutants were probed for Trs20p, Trs23p (TRAPP I core protein), Trs130p-HA (TRAPP II subunit) and Trs85p-HA (TRAPP III subunit). As seen in Figure 5A, Trs130p-HA levels were unaffected in *trs20D46Y* but were greatly reduced in *trs20ts* cells, suggesting destabilization of TRAPP II in the latter mutant. In addition, both mutants showed greatly reduced levels of Trs85p-HA. Only *trs20ts*, but not *trs20D46Y*, showed reduced Trs20p levels. Neither mutant displayed significant changes in the levels of Trs23p. These results suggest that the integrity of TRAPP III, but not TRAPP II, may be affected in *trs20D46Y*.

To examine this, we fractionated lysates on a Superose 6 column that we and others previously showed efficiently separates TRAPP I, II and III (12,37). The fractions from the column were probed with anti-Trs23p antibody. This protein is an integral component of the TRAPP I core and, thus, is found in all three TRAPP complexes. As previously reported for wild-type cells, Trs23p was detected in the fractions corresponding to TRAPP I, II and III (Figure 5B). In the *trs20D46Y* mutant there was a striking loss in the Trs23p signal in only the TRAPP III fractions. In contrast to *trs20D46Y*, the Trs23p signal in both TRAPP II and III was reduced in *trs20ts* (Figure 5B). Upon examination of Trs85p-HA, there was a decrease in this protein from the TRAPP peak in both *trs20D46Y* and *trs20ts*, consistent with the decrease in protein levels from whole cell lysates (Figure 5C). The results from the Superose 6 column suggest that TRAPP III is selectively destabilized in the *trs20D46Y* mutant. This destabilization may be due to a weakened interaction between Trs20p and Trs85p in this mutant (see Figure 3A).

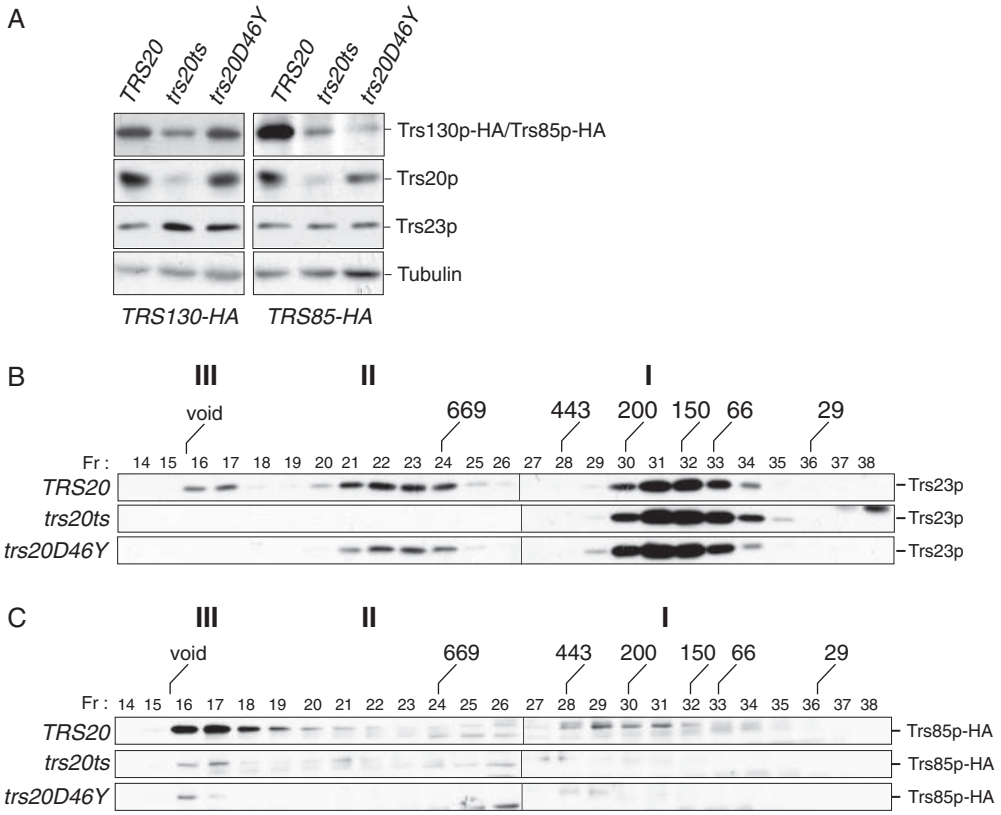

Figure 5: TRAPP III is destabilized in *trs20D46Y*. A) *TRS85* or *TRS130* was tagged with a 3XHA epitope in wild type, *trs20D46Y* and *trs20ts*. Lysates prepared from these strains were probed with anti-HA IgG, anti-Trs20p, anti-Trs23p and anti-tubulin (as a loading control). Lysates from the Trs85p-HA-tagged strains in (A) were fractionated on a Superose 6 size exclusion column in 300 mM NaCl and fractions were probed with (B) anti-Trs23p or (C) anti-HA (to detect Trs85p-HA) IgG. The location of the TRAPP I, II and III fractions is indicated as are the fractionation of molecular size standards.

Autophagy is defective in the trs20D46Y mutant

On the basis of the destabilization of TRAPP III, a complex involved in autophagy, we tested whether *trs20D46Y* affected autophagy. Growing cells in the presence or absence of a nitrogen source allow one to distinguish between the selective cytosol-to-vacuole (cvt) autophagic pathway (+nitrogen) and the non-selective pathway (−nitrogen). We first probed for the marker protein Ape1p, which uses the selective pathway in the presence of nitrogen but is transported to the vacuole in a non-selective manner in the absence of nitrogen (38). The processing of Ape1p is detected by examining the levels of the precursor form of the protein and the processed form that appears as a faster migrating species by SDS–PAGE using an Ape1p antibody. Consistent with the destabilization of TRAPP III in *trs20D46Y*, Ape1p processing in the presence of nitrogen was completely blocked when compared with wild type (Figure 6A, +N panel). In accordance with previous studies, *trs85*Δ and *atg1*Δ (a gene that is critical for autophagy) also showed blocks in the selective pathway (10,15) as did *trs20ts* (Figure 6A). In the absence of nitrogen, when Ape1p is processed by non-selective autophagy, a significant amount of mature Ape1p was detected in *trs20D46Y*, *trs20ts* and *trs85*Δ with small amounts of the precursor form also present, suggesting a defect in non-selective autophagy (Figure 6A, −N panel).

To further confirm autophagic defects in *trs20D46Y*, we examined the localization of Ape1p-GFP. In wild-type cells, a single punctum of fluorescence is often detected that represents Ape1p in the preautophagosomal structure (PAS) (39) (Figure 6B). Interestingly, *trs20D46Y* showed a single but much larger punctum of Ape1p-GFP

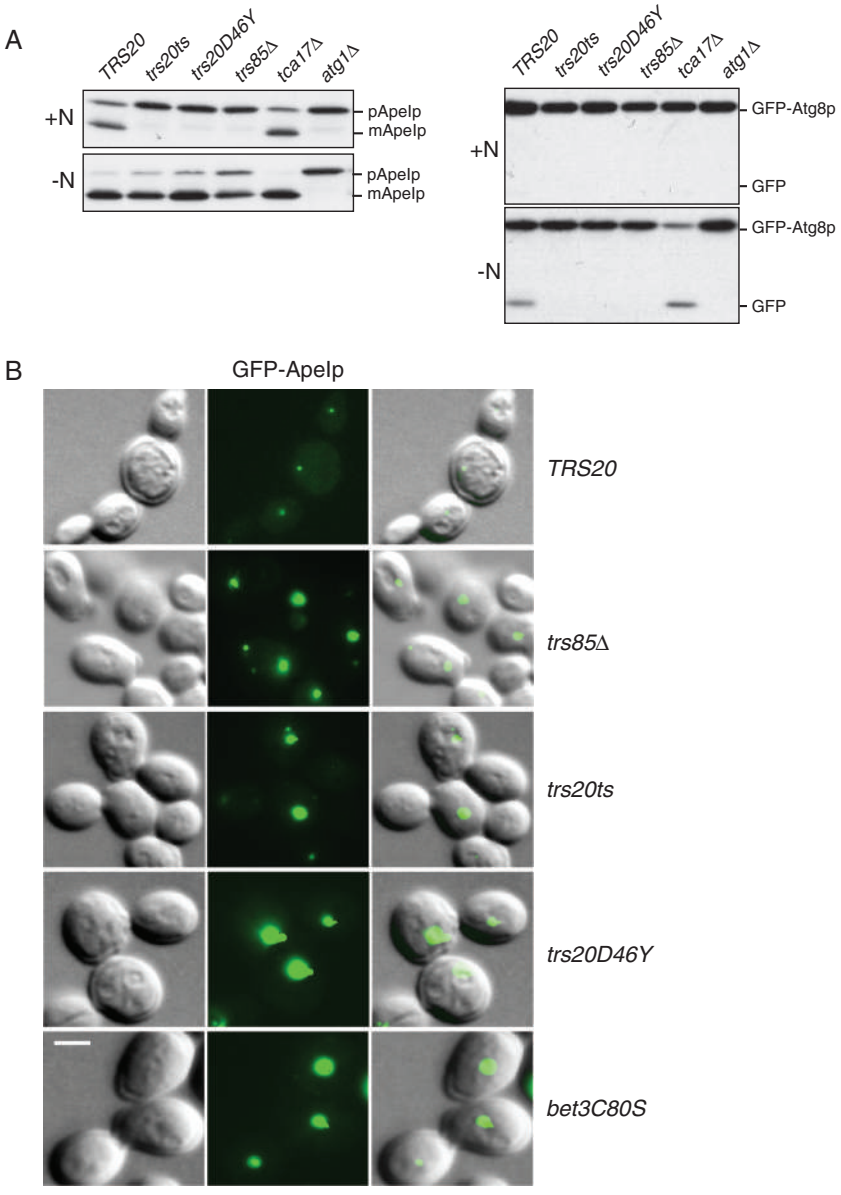

Figure 6: Both selective and non-selective autophagy are affected in *trs20D46Y*. A) The indicated yeast strains were grown in rich (+N; upper panel) or nitrogen starvation (−N; lower panel) medium as described in *Materials and Methods*. Equal amounts of protein were fractionated by SDS–PAGE and analyzed by western analysis using anti-Ape1p IgG or anti-GFP (to monitor GFP-Atg8p processing) as indicated. B) The strains indicated were transformed with GFP-Ape1p, fixed and visualized by fluorescence microscopy. The scale bar is 2 μm. Note the larger size of the GFP-Ape1p punctum in the mutants compared with wild type.

fluorescence, suggesting the protein accumulates in the PAS. This is consistent with the autophagic defect seen by western analysis above. Furthermore, *trs85*Δ and *trs20ts* also displayed a similar phenotype of a single, but much larger, punctum of fluorescence (Figure 6B). A single, large punctum such as that seen in *trs20D46Y* and *trs85*Δ has been reported in other mutants that block the cvt pathway (39).

To more carefully assess whether *trs20D46Y* affects non-selective autophagy, we examined the processing of GFP-Atg8p. Upon uptake into the vacuole under nitrogen starvation conditions, this fusion protein is cleaved, liberating GFP. This processing can be detected by western analysis. As seen in Figure 6A, *trs20D46Y* as well as *trs20ts* displayed a defect in GFP-Atg8p processing in nitrogen-starved medium (−N). A similar defect was also seen for *trs85*Δ, consistent with previous studies (14,15). Collectively, our results demonstrate that *trs20D46Y* affects both the selective (cvt) and non-selective autophagic pathways without affecting anterograde transport.

Trs20p and Tca17p have differing functions

Trs20p and its mammalian homolog C2 are phylogenetically and structurally related to a newly identified TRAPP-interacting protein called Tca17p in yeast (TRAPPC2L in higher eukaryotes) (25,28,33,34) (Protein Data Bank ID 3PR6). We therefore examined the interaction profile of Tca17p and the biochemical consequences in yeast of *tca17*Δ to that seen for Trs20p and *trs20D46Y*. By yeast two-hybrid analysis, and in accordance with our previously reported genetic interaction (25), when compared with the three TRAPP subunits whose interactions were affected by trs20D46Yp (i.e. Trs85p, Trs120p and Trs130p), we found that Tca17p only interacted with Trs130p (Figure S1, Supporting Information). In addition, size exclusion chromatography showed that *tca17*Δ altered the integrity of the TRAPP II peak but did not alter the integrity of the TRAPP III peak (Figure S2) (12). Finally, in contrast to *trs20D46Y*, *tca17*Δ blocked neither the processing of Ape1p in rich medium nor the processing of GFP-Atg8p in starvation medium (Figure 6A). While this latter result is in contradiction to that recently reported for *tca17ts* (14), it is noteworthy that our mutant is a simple *tca17* deletion when compared with *tca17ts*, which also includes modifications to *TRS120* and *TRS130*. In combination with our previous results showing that human C2, but not human C2L, could suppress *trs20*Δ (25), we suggest that Tca17p and Trs20p, although evolutionarily and structurally related, are functionally distinct.

The molecular size of TRAPP III depends upon membranes and Atg9p

The composition of TRAPP III differs from that of TRAPP I by the addition of a single subunit, Trs85p. However, the molecular size of TRAPP III (>1 MDa) is much greater than that of TRAPP I (∼200 kDa), and this difference cannot be accounted for by this single 85-kDa protein. A previous study did not identify any other polypeptides in this complex and oligomerization was also ruled out (12) (S.B. and M.S., unpublished observation). Suspecting that the large molecular size of TRAPP III was due to association with membranes, we examined the fractionation of Trs23p and Trs85p-HA in lysates prepared using Triton X-100. While Trs85p-HA shifted to a fraction with a smaller molecular size near TRAPP I, Trs23p spread out between the fractions spanning TRAPP III to II (Figure 7A). This spreading of the Trs23p peak in Triton X-100 was independent of Trs85p because a similar pattern was seen in *trs85*Δ treated with the detergent (Figure 7A). Such an effect was previously noted for Trs130p in a *tca17*Δ strain (12). As Trs23p is absent from the TRAPP III fractions in *trs85*Δ prepared without detergent (Figure S2), this result suggests that the fractionation of Trs23p seen in the presence of Triton X-100 is likely due to changes to TRAPP II. Our results indicate that, in the absence of detergent, TRAPP III is associated with Triton X-100-soluble membranes. Consistent with this notion, TRAPP III penetrated an Optiprep gradient further in the absence, when compared with the presence, of Triton X-100 (Figure 7B).

We next set out to identify a putative TRAPP III receptor on autophagic membranes by screening *atg*Δ mutants for changes in the fractionation pattern of TRAPP III on a size exclusion column. Our studies led us to focus on *atg9*Δ. In whole cell lysates, the levels of Trs85p-HA, but not Trs23p, were dramatically reduced upon nitrogen starvation in *atg9*Δ compared with wild type (Figure 7C, compare +/− nitrogen). Correspondingly, there was a decrease in the appearance of Trs85p-HA in the TRAPP III peak in nitrogen-starved *atg9*Δ cells relative to non-starved cells (Figure 7D). Remarkably, Trs23p was also reduced in the TRAPP III fractions (Figure 7D). This result is similar to that seen for *trs20D46Y* (see Figure 5) in which the cellular levels of Trs85p-HA, but not Trs23p, are reduced yet the amounts of both proteins in the TRAPP III fraction are greatly diminished. We next examined Atg17p because this protein has been reported to recruit Atg9p to autophagic membranes (40). In a nitrogen-starved *atg17*Δ strain, we did not detect a significant decrease in the levels of either Trs85p-HA or Trs23p relative to wild type (Figure 7C) and there were no differences in the fractionation of these proteins in the TRAPP III peak (Figure 7D) compared with non-starved cells. Collectively, our results suggest that the recruitment of TRAPP III during non-selective, but not during selective, autophagy requires Atg9p, and that an assembled TRAPP III complex is required for both selective and non-selective autophagy.

Palmitoylated Bet3p is enriched in TRAPP III

TRAPP III appears to be membrane associated, whereas TRAPP I is more easily separated from membranes because fractionation of the latter on a size exclusion column is not affected by detergent. What can account for this difference? The TRAPP I core subunit Bet3p was

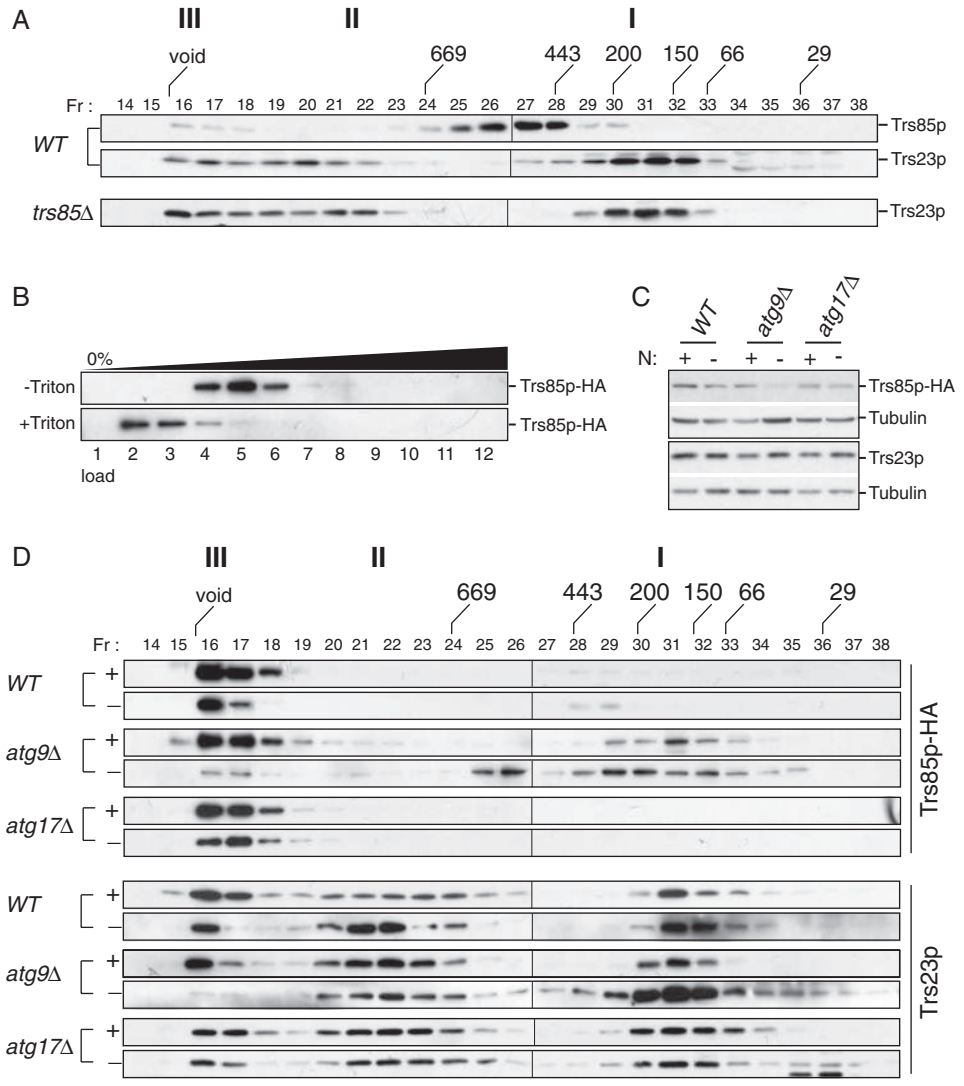

Figure 7: The molecular size of TRAPP III is dependent upon membranes and Atg9p. Lysate was prepared from (A) *TRS85*-HA or *trs85*Δ strains with 300 mM NaCl/1% Triton X-100. The lysates were fractionated on a Superose 6 size exclusion column. The fractions were probed for Trs23p and Trs85p-HA as indicated. B) Pooled fractions from a Superose 6 column enriched in TRAPP III derived from a *TRS85*-HA strain that was not treated with Triton X-100 were loaded on top of an Optiprep step gradient prepared as described in *Materials and Methods*. The top-loaded sample was either left untreated or incubated with 1% Triton X-100 before centrifugation on the gradient. Fractions were collected from the top of the gradient and probed for Trs85p-HA. C) Lysate in 300 mM NaCl was prepared from wild type, *atg9*Δ, *atg17*Δ, *atg9*Δ/*TRS85*-HA or *atg17*Δ/*TRS85*-HA grown in YPD (+) or nitrogen starvation medium (−). Lysates were probed for either Trs23p, Trs85p-HA or tubulin (as a loading control). D) A total of 2 mg of lysate from the cells in (C) was fractionated on a Superose 6 column and probed for Trs23p or Trs85p-HA as indicated.

shown to be lipid-modified by either palmitoylation or myristoylation (41,42). The modified cysteine residue at position 80 in the yeast protein is highly conserved yet, surprisingly, mutation of this residue does not lead to any observable growth phenotype. We speculated that lipid-modified Bet3p may partially account for the association of the TRAPP III complex with PAS membranes. If this is the case, *bet3C80S*, a mutant that prevents Bet3p palmitoylation (41–43), may block autophagy. Indeed, compared with wild type, *bet3C80S* displayed both a defect in Ape1p processing in the presence, but not the absence, of nitrogen and a starvation-induced reduction in GFP-Atg8p processing (Figure 8A). In addition, *bet3C80S* also displayed an enlarged Ape1p-GFP punctum similar to that seen for *trs85*Δ and *trs20D46Y* (Figure 6B). This suggests that palmitoylation of Bet3p is involved in the efficient functioning of TRAPP III in both selective and non-selective autophagy.

Given the results above, we speculated that palmitoylated Bet3p would be enriched in TRAPP III. To test this notion, a wild-type lysate was fractionated by size exclusion

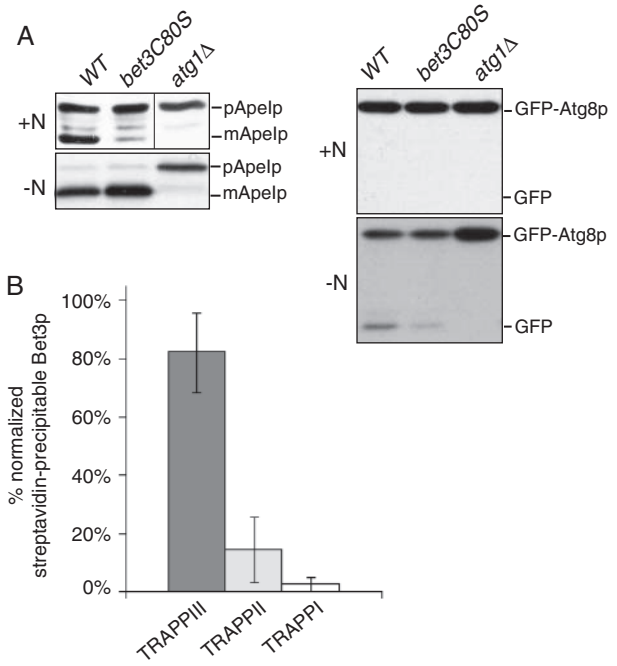

Figure 8: Lipidated Bet3p is enriched in TRAPP III. A) Lysates from wild type, *bet3C80S* and *atg1*Δ were prepared from cultures grown in YPD (+N) or nitrogen starvation (−N) medium as described in *Materials and Methods* and analyzed by western analysis with anti-Ape1p IgG or anti-GFP (to monitor GFP-Atg8p processing) as indicated. B) A wild-type lysate was fractionated on a Superose 6 column and the peak of TRAPP I, II and III was pooled individually and subjected to acyl–biotin exchange as described in *Materials and Methods*. A portion of each input fraction, to enable normalization to Bet3p, along with the entire precipitate from the streptavidin-agarose beads was subjected to western analysis using anti-Bet3p serum and quantitated using Image J. Error bars indicate standard deviation.

chromatography and the fractions containing TRAPP I, II and III were pooled separately and subjected to acyl–biotin exchange. In this assay, acyl chains on proteins are exchanged for a biotin moiety, which can then bind to streptavidin-agarose beads. Precipitation of proteins onto the beads indicates that the proteins were initially acylated. As shown in Figure 8B, after normalization to Bet3p levels in the input, acylated Bet3p was greatly enriched in TRAPP III. Our results suggest that acylated Bet3p is important for the function and/or localization of the TRAPP III complex.

Discussion

Here, we demonstrate that the mammalian TRAPP protein C2 binds to the SNARE protein Syntaxin 5. This interaction is weakened by the pathogenic D47Y mutation in C2 and led us to speculate that a yeast mutation patterned after this mutation in the C2 homolog Trs20p would affect early secretory pathway traffic. Instead, this yeast mutant (*trs20D46Y*) did not display anterograde trafficking defects but was defective in the selective (cvt) and non-selective autophagy pathways. In addition, *trs20D46Y*, *atg9*Δ and *bet3C80S* mutants revealed complexities in the organization and function of the TRAPP III complex that is involved in these pathways. It should be stressed that although the *trs20* mutants examined in this study did not display trafficking defects in the early secretory pathway, other residues in this protein may in fact impinge on this process.

Complexities in TRAPP III assembly and function

The subunit composition of TRAPP III differs from TRAPP I by just a single additional protein (Trs85p in TRAPP III), yet the molecular size of TRAPP III is much greater than that of TRAPP I (see Figures 5 and 7) (12,37) and this is not due to oligomerization of Trs85p/TRAPP III (12) (S.B. and M.S., unpublished observation). We found that the cellular levels of the TRAPP III-specific protein Trs85p-HA, but not the TRAPP I core protein Trs23p, were greatly diminished in *trs20D46Y* as well as in *atg9*Δ, but unaffected in *atg17*Δ relative to wild type. The former two mutants showed reduced levels of both Trs85p-HA and Trs23p in the TRAPP III fractions. Our results imply that, during non-selective autophagy, the recruitment of TRAPP III to autophagic membranes is dependent upon Atg9p (Figure 9A). Our data do not address which, if any, subunit of TRAPP III interacts directly with Atg9p. However, a recent report suggested that Trs85p, but not other TRAPP I core subunits, binds directly to Atg9p and its localization is affected in *atg9*Δ cells (44). If this is the case, our results with *trs20D46Y* suggest that recruitment of the TRAPP I core to the Atg9p-Trs85p unit is mediated in part by Trs20p and particularly by its conserved D46 residue. Our data leave open the possibility that the TRAPP I core may be recruited to membranes distinct from those containing Trs85p in which case their interaction to form TRAPP III may contribute to tethering (Figure 9B). This would be similar to the mechanism of exocyst complex-mediated tethering in which vesicles are tethered to the plasma membrane via interactions between exocyst components on separate membranes (45). As the cellular levels of Trs85p-HA and the appearance of Trs85p-HA and Trs23p in TRAPP III were not affected under rich growth conditions in *atg9*Δ, recruitment of TRAPP III to autophagic membranes during selective autophagy must be dependent on an as yet unidentified factor (Figure 9C).

Our results provide a clue as to the role of *trs20D46Y* in autophagy. Based on Ape1p processing in rich medium, this mutant affects the cvt pathway. While there was only a minor defect in Ape1p processing under nitrogen-starved conditions, examination of GFP-Atg8p under these conditions indicated that non-selective autophagy was also strongly affected. A similar phenotype consisting of a mild defect of Ape1p processing but a strong defect in GFP-Atg8p processing in starvation conditions has been reported for the TRAPP mutant *trs85*Δ as well as for *vac8*Δ (14,15,46). In the latter mutant, autophagic bodies were reduced in both number and size. Our results,

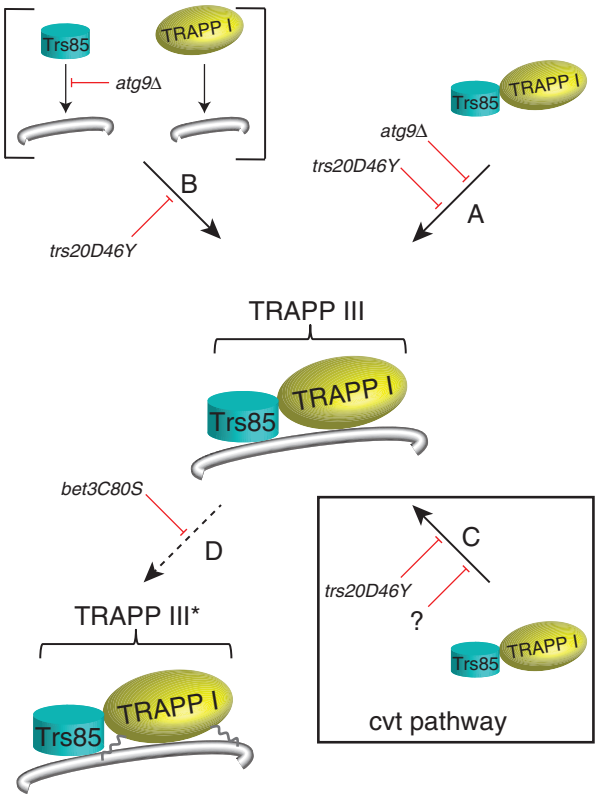

Figure 9: Model for the organization and assembly of TRAPP III. Assembly of TRAPP III is dependent upon an interaction between Trs20p and Trs85p and is mediated by the conserved D46 residue in Trs20p. Assembled TRAPP III is then recruited to autophagic membranes in an Atg9p-dependent manner (A). This may be mediated by a direct interaction between Trs85p and Atg9p as recently suggested (44). Alternatively, Trs85p and Trs23p may be recruited to separate membranes, and their interaction to form TRAPP III is mediated by the same Trs20p–Trs85p interaction described above (B). Note that the involvement of Atg9p in this scenario is based on a recent study (44). Although TRAPP III assembly in the selective (cvt) pathway is also mediated by a Trs20p–Trs85p interaction, recruitment to autophagic membranes does not appear to require Atg9p and some as yet unknown factor (denoted as ?) may be involved (C). In both cases (selective and non-selective autophagy) lipidation of Bet3p in TRAPP III increases the functional efficiency of the TRAPP III complex (denoted by TRAPP III*). The steps that are blocked by the various mutants used in this study are indicated by red lines.

therefore, suggest that in *trs20D46Y* cvt vesicles fail to form. However, in nitrogen-starved conditions, while some autophagosomes may form, their size is likely to be abnormally small.

What is the role of Bet3p lipidation in TRAPP III function? The enrichment of lipidated Bet3p in TRAPP III and the fact that TRAPP III remains membrane associated in *bet3C80S* (S.B. and M.S., unpublished observation) suggest that lipidation alone cannot account for TRAPP III membrane attachment. It is tempting to speculate that lipidated Bet3p may localize the complex to a membrane sub-domain of autophagic vesicles. It is noteworthy that acylation of proteins is one mechanism that directs their intracellular localization (47,48). Alternatively, lipidation of Bet3p/TRAPPC3 has been postulated to alter its structure (42,43,49), which may promote binding to these specialized membrane regions or increase the efficiency of TRAPP III function (Figure 9D).

Trs20p as an adaptor protein

When compared with *tca17*Δ, our results with *trs20D46Y* suggest that Trs20p can act as an adaptor protein for the TRAPP II-specific subunit Trs120p and the TRAPP III-specific subunit Trs85p. This adaptor function of Trs20p is similar to that reported for the mammalian homolog C2 (35). As Trs85p and Trs120p do not reside in the same complex, their interaction with Trs20p is not mutually exclusive. The fact that the D46Y mutation in Trs20p weakens both interactions suggests that these two TRAPP subunits interact with Trs20p in a similar fashion. The suggestion that Trs120p binds directly to Trs20p is in disagreement with the recently published electron microscopic structure of the TRAPP II complex, which suggested that Trs20p was in direct contact with Trs130p, whereas Trs120p was on a side of the complex opposite to that of Trs20p (50). While our results leave this possibility open, we do not believe this to be the case for the following reasons. The interaction between Trs20p and Trs130p is much weaker than that between Trs20p and Trs120p (M.S., unpublished observation). In addition, the similarity in structure between Trs20p and Tca17p leaves open the possibility that some Trs20p interactions occur owing to the similar structure between these two proteins and do not take place *in vivo*. Indeed, Tca17p was found to bind only to Trs130p, which is consistent with a previous study showing that Tca17p binds to the amino-terminus of Trs130p (12) and our earlier result showing a strong genetic interaction between *TCA17* and *TRS130* (25). We suggest that Tca17p may be the TRAPP subunit that interacts with Trs130p, whereas Trs20p acts as an adaptor to allow either Trs85p or Trs120p to interact with the TRAPP I core complex. It remains unclear how Tca17p interacts with the TRAPP I core and how it is excluded from TRAPP III.

Implications for SEDT

The C2D47Y mutation was identified in a patient with SEDT (22). A recent study suggested that C2 (called sedlin) regulates the Sar1 GTPase cycle at ER exit sites to allow ER-derived carriers to grow to a size that can accommodate large cargo such as collagen (24). It is the transport of procollagen that is believed to be defective in SEDT patients. Although we could not detect an interaction between Trs20p and the yeast Syntaxin 5 homolog Sed5p, it is possible that the mammalian Trs20p homolog C2 evolved the ability to interact with Syntaxin 5. In this case, procollagen release from the Golgi in

patients with the C2D47Y mutation may not be affected but fusion of the megacarriers with the Golgi would be defective. Alternatively, Syntaxin 5 has been implicated in membrane traffic steps beyond the ER-to-Golgi portion of the secretory pathway including the endocytic pathway (51,52) and procollagen transport in patients with the C2D47Y mutation may be blocked at these later stages. It is noteworthy that defects in endocytosis could indirectly block anterograde transport, suggesting that the C2D47Y mutation may have an indirect effect on procollagen transport. At present, it is difficult to envision how a defect in autophagy could affect procollagen transport. Studies on the role of mammalian C2 in both endocytosis and autophagy will help address these possibilities.

Materials and Methods

Yeast strains and molecular biological techniques

All yeast strains were constructed using standard genetic techniques. *TRS20* mutations were introduced by site-directed mutagenesis using High-Fidelity Polymerase (Roche) and expressed in yeast under the endogenous *TRS20* promoter from a single-copy plasmid (pRS315 or pRS316). The C2D47Y mutation was constructed as above and cloned into the pRK5-myc plasmid facilitating detection of the mutant protein with anti-myc antibody. For yeast two-hybrid analysis, open reading frames were inserted into pGBKT7 or pGADT7 using either restriction enzyme cloning or Gateway cloning into modified, Gateway-compatible vectors (53).

Yeast two-hybrid analysis

Yeast cells (AH109 and Y187) were transformed with either pGBKT7 or pGADT7 constructs. The cells were mated overnight on YPD plates and then replicated to selective medium (-leucine/-tryptophan, -leucine/-tryptophan/-histidine ± 2 mM 3-aminotriazole, -leucine/-tryptophan/-histidine/-adenine) to ensure that both plasmids were present and to test for an interaction. Growth was monitored daily for up to 8 days.

Cell culture and immunoprecipitation

HeLa and 293T cells were maintained in a humidified environment with 5% CO_2 at 37°C. Transfections were performed using the Ca_2PO_4 method and 10 μg of plasmid DNA per 10-cm dish. In certain cases, cells were treated with 10 μM NEM during the time course indicated in Figure 1. For immunoprecipitations, 500 μg of lysate prepared in lysis buffer [150 mM NaCl, 50 mM Tris, pH 7.2, 1 mM DTT, 1% Triton X-100, 0.5 mM ethylenediaminetetraacetic acid and 1 mini-tablet of protease inhibitor cocktail (Roche) per 10 mL] was incubated with 0.4 μg of anti-Syntaxin 5 antibody (Santa Cruz) overnight on ice. The sample was then incubated with a 10 μL bed volume of protein A-agarose beads for 60 min in the cold. The beads were washed thrice with lysis buffer and eluted by boiling with 25 μL SDS–PAGE sample buffer.

Yeast trafficking assays

The assay for CPY transport and GFP-Snc1p localization were performed as previously described (37). For the CPY assay the cells were shifted to 37°C for 60 min.

For the general secretion assay, two OD_{600} units of cells were preshifted to 37°C for 30 min. The cells were then pulse-labeled with 100 μCi ^{35}S-methionine/cysteine for 15 min and chased with 10 mM unlabeled methionine and cysteine for 15 min. Before pelleting the cells NaN_3/NaF was added to the culture to a final concentration of 0.5 mM. The cells were pelleted and the growth medium was precipitated with 10% trichloroacetic acid on ice. The pellet was dissolved in SDS–PAGE sample buffer and fractionated by SDS–PAGE.

CFW growth was monitored by spotting serial dilutions of cells on YPD ± 10 μg/mL CFW and incubating the plates at 30°C. Growth was monitored daily for up to 5 days.

Processing of pre-Ape1p was performed by monitoring the forms of the protein using western analysis (54). Cells were grown overnight to an $OD_{600} \leq 1$ in YPD and resuspended in prewarmed YPD medium at 37.5°C (for heat-sensitive mutants) or 30°C for 1 h. For selective autophagy cells were immediately processed for lysis (see below). For non-selective autophagy cells were pelleted, washed in water and resuspended in prewarmed synthetic medium lacking nitrogen, incubated for 2–4 h at 37.5°C (for heat-sensitive mutants) or 30°C and then processed for lysis. Localization of GFP-Ape1p was performed on fixed cells according to the GFP-Snc1p protocol above.

Preparation of yeast cell lysates

Lysates for size exclusion chromatography were prepared as previously described (37) and 2–5 mg of total protein was fractionated on a Superose 6 column. In some cases, 1% Triton X-100 was added to the lysis buffer and was included in the size exclusion column buffer. For pre-Ape1p processing, lysates were prepared by converting the cells to spheroplasts in medium containing 1.4 M sorbitol, 50 mM KP_i, pH 7.5, 36 mM β-mercaptoethanol and 33 μg/mL zymolyase 100T for 30 min at 37.5°C. Spheroplasts were lysed in 1% SDS, boiled and cleared by centrifugation.

Optiprep gradient assay

A yeast lysate from *TRS85*-HA cells was prepared in the absence of detergent and fractionated on a Superose 6 column as described (37). Fractions containing TRAPP III were pooled and a portion was supplemented with 1% Triton X-100 before incubating on ice for 30 min. A sample (100 μL) was combined with size exclusion column buffer to a final volume of 300 μL and then loaded on top of a step Optiprep gradient composed of 1 mL 15%, 1 mL 30%, 1 mL 40%, 0.8 mL 45% and 1.2 mL 54% Optiprep. The sample was centrifuged in an SW55 rotor at 157 000 × g for 16 h. Fractions were collected from the top of the tube and probed for Trs85p-HA with anti-HA antibody.

Recombinant protein expression and in vitro binding

Syntaxin 5 (amino acids 1-333) was recombined into pDEST15 (GST fusion vector) from a Gateway entry clone. C2 and C2D47Y were recombined into pDEST17 (His fusion vector) from Gateway entry clones. Protein was expressed by inducing with 1 mM Isopropyl β-D-1-thiogalactopyranoside in BL21(DE3) cells overnight at 25°C. The protein was purified on glutathione-agarose resin or Ni^{2+}-NTA resin as per manufacturer's instructions.

In vitro binding assays contained 0.5 μM of GST-Syntaxin 5 with increasing amounts (0, 0.1, 0.2 and 0.5 μM) of His-tagged C2 wild type or D47Y. Samples were made up to a total volume of 250 μL with 1× binding buffer (10 mM HEPES, pH 7.4, 25 mM NaCl, 115 mM KCl, 2 mM $MgCl_2$ and 0.1% Triton X-100) and left on ice at 4°C for 1 h to allow binding. Pulldown employed 10 μL glutathione-agarose resin (GE Healthcare) in the cold for 1 h. Samples were washed thrice with binding buffer and eluted by boiling with SDS–PAGE sample buffer. Western blotting was performed using horseradish peroxidase-conjugated anti-His antibody (Qiagen).

Acyl–biotin exchange

Biotinylation of acylated proteins was performed essentially as described (55,56) with minor modifications. A wild-type yeast lysate was prepared in the absence of detergent and fractionated on a Superose 6 column as described (37). Fractions containing TRAPP I, II and III were separately pooled and incubated at 4°C for 30 min in 1% Triton X-100 with 25 mM NEM. The proteins were precipitated twice using

methanol/chloroform and resuspended in buffer A (2% SDS, 8 M urea, 100 mM NaCl and 50 mM Tris-HCl, pH 7.4). Six volumes of a solution containing 1 M hydroxylamine and 300 μM biotin-BMCC (Pierce) was added and incubated for 2 h at 4°C. The proteins were precipitated once using methanol/chloroform, resuspended in 100 μL of buffer A, then diluted to 1 mL with PBS containing 5mM EDTA and 0.1% Triton X-100 and incubated with 15 μL of streptavidin-agarose beads (Sigma) for 1 h at room temperature. The beads were washed in PBS containing 0.5 M NaCl and 0.1% Triton X-100 after which the proteins were eluted by boiling in a 3:1 mix of buffer A:4× SDS–PAGE sample buffer. Bet3p was detected by western analysis using anti-Bet3p IgG.

Acknowledgments

We are grateful to Drs Daniel Klionsky, Vladimir Titorenko, Christopher Brett and Jesse Hay for reagents, and to Annika Seddon for technical assistance. We also thank Dr Daniel Klionsky for helpful discussions and Rodney Joyette for the artwork in Figure 9. S. B. is a recipient of a studentship from the Fonds de Recherche du Québec - Nature et Technologies. M. S. is supported by grants from the Canadian Institutes of Health Research, the Natural Sciences and Engineering Council of Canada and the Canada Foundation for Innovation. M. S. is a member of the Groupe de Recherche Axé sur la Structure des Protéines (GRASP).

Supporting Information

Additional Supporting Information may be found in the online version of this article:

Figure S1. Tca17p interacts with Trs130p, but not with Trs120p or Trs85p. The open reading frame encoding *TCA17* was cloned into pGBKT7, transformed into AH109 yeast cells and mated to Y187 yeast that harbored pGADT7 containing the open reading frame for either *TRS130*, *TRS120* or *TRS85*. Growth on SD-leu/-trp/-his/-ade indicates that Tca17p binds to only Trs130p. This figure is related to Figure 3A.

Figure S2. Fractionation of Trs23p in *trs85*Δ and *tca17*Δ. Lysate prepared from *tca17*Δ or *trs85*Δ was fractionated on a Superose 6 size exclusion column in 300 mM NaCl. The peaks for TRAPP I, II and III are indicated. Also shown is the same wild-type blot shown in Figure 5 for comparison. The Trs23p signal in the TRAPP II fractions is missing but remains in the TRAPP III fractions. This figure is related to Figures 5B and 7A.

References

1. Aridor M, Hannan LA. Traffic jam: a compendium of human diseases that affect intracellular transport processes. Traffic 2000;1:836–851.
2. Aridor M, Hannan LA. Traffic jams II: an update of diseases of intracellular transport. Traffic 2002;3:781–790.
3. Cai H, Reinisch K, Ferro-Novick S. Coats, tethers, Rabs, and SNAREs work together to mediate the intracellular destination of a transport vesicle. Dev Cell 2007;12:671–682.
4. Cai H, Yu S, Menon S, Cai Y, Lazarova D, Fu C, Reinisch K, Hay JC, Ferro-Novick S. TRAPPI tethers COPII vesicles by binding the coat subunit Sec23. Nature 2007;445:941–944.
5. Lord C, Bhandari D, Menon S, Ghassemian M, Nycz D, Hay J, Ghosh P, Ferro-Novick S. Sequential interactions with Sec23 control the direction of vesicle traffic. Nature 2011;473:181–186.
6. Jones S, Newman C, Liu F, Segev N. The TRAPP complex is a nucleotide exchanger for Ypt1 and Ypt31/32. Mol Biol Cell 2000;11:4403–4411.
7. Wang W, Sacher M, Ferro-Novick S. TRAPP stimulates guanine nucleotide exchange on Ypt1p. J Cell Biol 2000;151:289–296.
8. Rossi G, Kolstad K, Stone S, Palluault F, Ferro-Novick S. BET3 encodes a novel hydrophilic protein that acts in conjunction with yeast SNAREs. Mol Biol Cell 1995;6:1769–1780.
9. Sacher M, Barrowman J, Wang W, Horecka J, Zhang Y, Pypaert M, Ferro-Novick S. TRAPP I implicated in the specificity of tethering in ER-to-Golgi transport. Mol Cell 2001;7:433–442.
10. Lynch-Day MA, Bhandari D, Menon S, Huang J, Cai H, Bartholomew CR, Brumell JH, Ferro-Novick S, Klionsky DJ. Trs85 directs a Ypt1 GEF, TRAPPIII, to the phagophore to promote autophagy. Proc Natl Acad Sci U S A 2010;107:7811–7816.
11. Montpetit B, Conibear E. Identification of the novel TRAPP associated protein Tca17. Traffic 2009;10:713–723.
12. Choi C, Davey M, Schluter C, Pandher P, Fang Y, Foster LJ, Conibear E. Organization and assembly of the TRAPPII complex. Traffic 2011;12:715–725.
13. Cai H, Zhang Y, Pypaert M, Walker L, Ferro-Novick S. Mutants in trs120 disrupt traffic from the early endosome to the late Golgi. J Cell Biol 2005;171:823–833.
14. Zou S, Chen Y, Liu Y, Segev N, Yu S, Liu Y, Min G, Ye M, Zeng Y, Zhu X, Hong B, Bjorn LO, Liang Y, Li S, Xie Z. Trs130 participates in autophagy through GTPases Ypt31/32 in *Saccharomyces cerevisiae*. Traffic 2013;14:233–246.
15. Meiling-Wesse K, Epple UD, Krick R, Barth H, Appelles A, Voss C, Eskelinen EL, Thumm M. Trs85 (Gsg1), a component of the TRAPP complexes, is required for the organization of the preautophagosomal structure during selective autophagy via the Cvt pathway. J Biol Chem 2005;280:33669–33678.
16. Lipatova Z, Belogortseva N, Zhang XQ, Kim J, Taussig D, Segev N. Regulation of selective autophagy onset by a Ypt/Rab GTPase module. Proc Natl Acad Sci U S A 2012;109:6981–6986.
17. Zou S, Liu Y, Zhang XQ, Chen Y, Ye M, Zhu X, Yang S, Lipatova Z, Liang Y, Segev N. Modular TRAPP complexes regulate intracellular protein trafficking through multiple Ypt/Rab GTPases in *Saccharomyces cerevisiae*. Genetics 2012;191:451–460.
18. Bacon RA, Salminen A, Ruohola H, Novick P, Ferro-Novick S. The GTP-binding protein Ypt1 is required for transport in vitro: the Golgi apparatus is defective in ypt1 mutants. J Cell Biol 1989;109:1015–1022.
19. Jedd G, Richardson C, Litt R, Segev N. The Ypt1 GTPase is essential for the first two steps of the yeast secretory pathway. J Cell Biol 1995;131:583–590.
20. Sclafani A, Chen S, Rivera-Molina F, Reinisch K, Novick P, Ferro-Novick S. Establishing a role for the GTPase Ypt1p at the late Golgi. Traffic 2010;11:520–532.
21. Segev N, Mulholland J, Botstein D. The yeast GTP-binding YPT1 protein and a mammalian counterpart are associated with the secretion machinery. Cell 1988;52:915–924.
22. Shaw MA, Brunetti-Pierri N, Kadasi L, Kovacova V, Van ML, De BD, Salerno M, Gecz J. Identification of three novel SEDL mutations, including mutation in the rare, non-canonical splice site of exon 4. Clin Genet 2003;64:235–242.
23. Tiller GE, Hannig VL, Dozier D, Carrel L, Trevarthen KC, Wilcox WR, Mundlos S, Haines JL, Gedeon AK, Gecz J. A recurrent RNA-splicing mutation in the SEDL gene causes X-linked spondyloepiphyseal dysplasia tarda. Am J Hum Genet 2001;68:1398–1407.
24. Venditti R, Scanu T, Santoro M, Di TG, Spaar A, Gaibisso R, Beznoussenko GV, Mironov AA, Mironov A, Jr., Zelante L, Piemontese MR, Notarangelo A, Malhotra V, Vertel BM, Wilson C. Sedlin controls the ER export of procollagen by regulating the Sar1 cycle. Science 2012;337:1668–1672.
25. Scrivens PJ, Shahrzad N, Moores A, Morin A, Brunet S, Sacher M. TRAPPC2L is a novel, highly conserved TRAPP-interacting protein. Traffic 2009;10:724–736.
26. Gecz J, Shaw MA, Bellon JR, de Barros LM. Human wild-type SEDL protein functionally complements yeast Trs20p but some naturally occurring SEDL mutants do not. Gene 2003;320:137–144.
27. Gonzalez LC Jr, Weis WI, Scheller RH. A novel snare N-terminal domain revealed by the crystal structure of Sec22b. J Biol Chem 2001;276:24203–24211.
28. Jang SB, Kim YG, Cho YS, Suh PG, Kim KH, Oh BH. Crystal structure of SEDL and its implications for a genetic disease spondyloepiphyseal dysplasia tarda. J Biol Chem 2002;277:49863–49869.
29. Tochio H, Tsui MM, Banfield DK, Zhang M. An autoinhibitory mechanism for nonsyntaxin SNARE proteins revealed by the structure of Ykt6p. Science 2001;293:698–702.

30. Williams AL, Ehm S, Jacobson NC, Xu D, Hay JC. rsly1 binding to syntaxin 5 is required for endoplasmic reticulum-to-Golgi transport but does not promote SNARE motif accessibility. Mol Biol Cell 2004;15:162–175.
31. Stevens T, Esmon B, Schekman R. Early stages in the yeast secretory pathway are required for transport of carboxypeptidase Y to the vacuole. Cell 1982;30:439–448.
32. Ben-Aroya S, Coombes C, Kwok T, O'Donnell KA, Boeke JD, Hieter P. Toward a comprehensive temperature-sensitive mutant repository of the essential genes of *Saccharomyces cerevisiae*. Mol Cell 2008;30:248–258.
33. Cai Y, Chin HF, Lazarova D, Menon S, Fu C, Cai H, Sclafani A, Rodgers DW, De La Cruz EM, Ferro-Novick S, Reinisch KM. The structural basis for activation of the Rab Ypt1p by the TRAPP membrane-tethering complexes. Cell 2008;133:1202–1213.
34. Kim YG, Raunser S, Munger C, Wagner J, Song YL, Cygler M, Walz T, Oh BH, Sacher M. The architecture of the multisubunit TRAPP I complex suggests a model for vesicle tethering. Cell 2006;127:817–830.
35. Zong M, Wu XG, Chan CW, Choi MY, Chan HC, Tanner JA, Yu S. The adaptor function of TRAPPC2 in mammalian TRAPPs explains TRAPPC2-associated SEDT and TRAPPC9-associated congenital intellectual disability. PLoS One 2011;6:e23350.
36. Valdivia RH, Baggott D, Chuang JS, Schekman RW. The yeast clathrin adaptor protein complex 1 is required for the efficient retention of a subset of late Golgi membrane proteins. Dev Cell 2002;2:283–294.
37. Brunet S, Noueihed B, Shahrzad N, Saint-Dic D, Hasaj B, Guan TL, Moores A, Barlowe C, Sacher M. The SMS domain of Trs23p is responsible for the in vitro appearance of the TRAPP I complex in *Saccharomyces cerevisiae*. Cell Logist 2012;2:28–42.
38. Scott SV, Hefner-Gravink A, Morano KA, Noda T, Ohsumi Y, Klionsky DJ. Cytoplasm-to-vacuole targeting and autophagy employ the same machinery to deliver proteins to the yeast vacuole. Proc Natl Acad Sci U S A 1996;93:12304–12308.
39. Shintani T, Huang WP, Stromhaug PE, Klionsky DJ. Mechanism of cargo selection in the cytoplasm to vacuole targeting pathway. Dev Cell 2002;3:825–837.
40. Sekito T, Kawamata T, Ichikawa R, Suzuki K, Ohsumi Y. Atg17 recruits Atg9 to organize the pre-autophagosomal structure. Genes Cells 2009;14:525–538.
41. Kim YG, Sohn EJ, Seo J, Lee KJ, Lee HS, Hwang I, Whiteway M, Sacher M. Crystal structure of bet3 reveals a novel mechanism for Golgi localization of tethering factor TRAPP. Nat Struct Mol Biol 2005;12:38–45.
42. Turnbull AP, Kummel D, Prinz B, Holz C, Schultchen J, Lang C, Niesen FH, Hofmann KP, Delbruck H, Behlke J, Muller EC, Jarosch E, Sommer T, Heinemann U. Structure of palmitoylated BET3: insights into TRAPP complex assembly and membrane localization. EMBO J 2005;24:875–884.
43. Kummel D, Heinemann U, Veit M. Unique self-palmitoylation activity of the transport protein particle component Bet3: a mechanism required for protein stability. Proc Natl Acad Sci U S A 2006;103:12701–12706.
44. Kakuta S, Yamamoto H, Negishi L, Kondo-Kakuta C, Hayashi N, Ohsumi Y. Atg9 vesicles recruit vesicle-tethering proteins, Trs85 and Ypt1, to the autophagosome formation site. J Biol Chem 2012;287:44261–44269.
45. Boyd C, Hughes T, Pypaert M, Novick P. Vesicles carry most exocyst subunits to exocytic sites marked by the remaining two subunits, Sec3p and Exo70p. J Cell Biol 2004;167:889–901.
46. Cheong H, Yorimitsu T, Reggiori F, Legakis JE, Wang CW, Klionsky DJ. Atg17 regulates the magnitude of the autophagic response. Mol Biol Cell 2005;16:3438–3453.
47. Munro S. The Golgi apparatus: defining the identity of Golgi membranes. Curr Opin Cell Biol 2005;17:395–401.
48. Roskoski R Jr. Protein prenylation: a pivotal posttranslational process. Biochem Biophys Res Commun 2003;303:1–7.
49. Kummel D, Walter J, Heck M, Heinemann U, Veit M. Characterization of the self-palmitoylation activity of the transport protein particle component Bet3. Cell Mol Life Sci 2010;67:2653–2664.
50. Yip CK, Berscheminski J, Walz T. Molecular architecture of the TRAPPII complex and implications for vesicle tethering. Nat Struct Mol Biol 2010;17:1298–1304.
51. Tai G, Lu L, Wang TL, Tang BL, Goud B, Johannes L, Hong W. Participation of the syntaxin 5/Ykt6/GS28/GS15 SNARE complex in transport from the early/recycling endosome to the trans-Golgi network. Mol Biol Cell 2004;15:4011–4022.
52. Xu Y, Martin S, James DE, Hong W. GS15 forms a SNARE complex with syntaxin 5, GS28, and Ykt6 and is implicated in traffic in the early cisternae of the Golgi apparatus. Mol Biol Cell 2002;13:3493–3507.
53. Scrivens PJ, Noueihed B, Shahrzad N, Hul S, Brunet S, Sacher M. C4orf41 and TTC-15 are mammalian TRAPP components with a role at an early stage in ER-to-Golgi trafficking. Mol Biol Cell 2011;22:2083–2093.
54. Klionsky DJ, Cueva R, Yaver DS. Aminopeptidase I of *Saccharomyces cerevisiae* is localized to the vacuole independent of the secretory pathway. J Cell Biol 1992;119:287–299.
55. Hou H, Subramanian K, LaGrassa TJ, Markgraf D, Dietrich LE, Urban J, Decker N, Ungermann C. The DHHC protein Pfa3 affects vacuole-associated palmitoylation of the fusion factor Vac8. Proc Natl Acad Sci U S A 2005;102:17366–17371.
56. Wan J, Roth AF, Bailey AO, Davis NG. Palmitoylated proteins: purification and identification. Nat Protoc 2007;2:1573–1584.

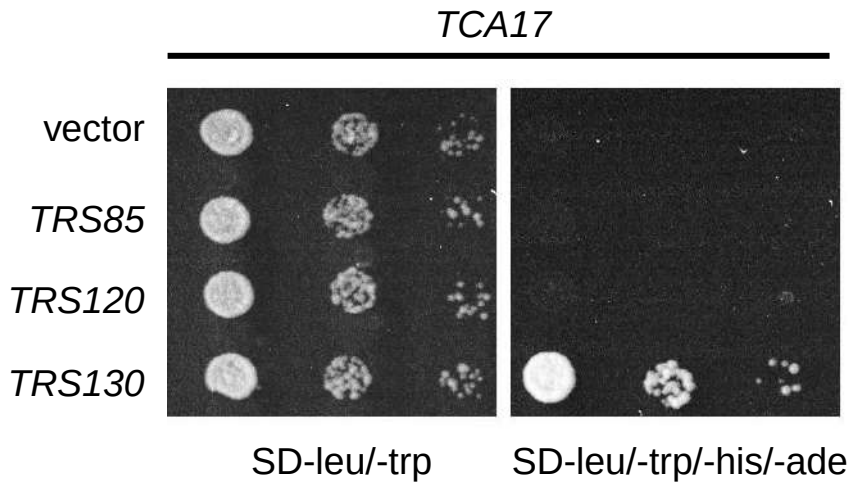

Supplemental Figure S1

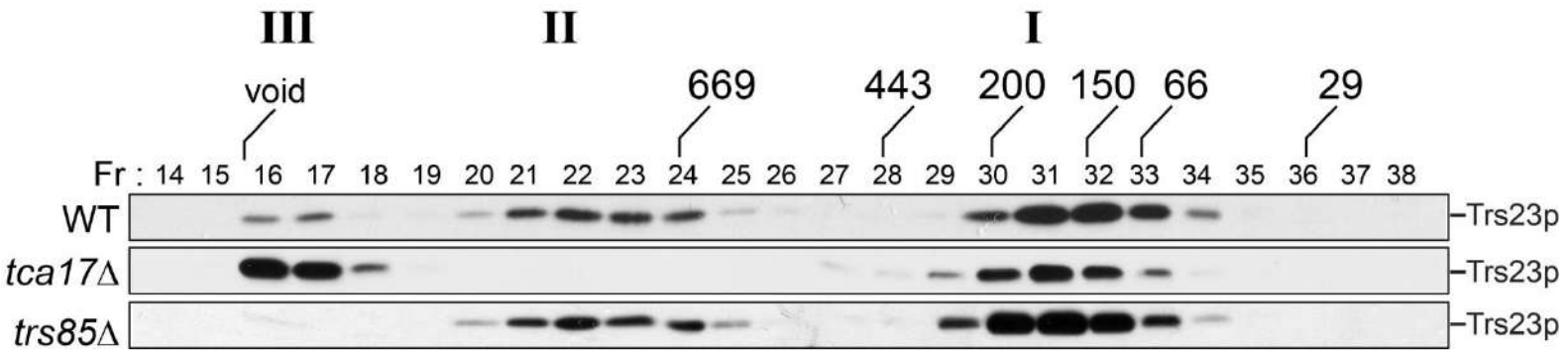

Supplemental Figure S2